Supplementary Information for "Ultra-Stable Weyl Topology Driven by Magnetic Textures in the Shandite Compound $Co_3Sn_2S_{(2-x)}Se_x$"

Dang Khoa Le[1*†], Eklavya Thareja[1*†], Bektur Konushbaev[1†], Gina Pantano[1†], Tom Saunderson[2,3†], Manh-Huong Phan[1,4†], Yuriy Mokrousov[2,5†], Jacob Gayles[1†]

[1*]Department of Physics, University of South Florida, Tampa, 33620, USA.
[2]Peter Grünberg Institut and Institute for Advanced Simulation, Forschungszentrum Jülich and JARA, 52425, Jülich, Germany.
[3]Institut für Physik and Halle-Berlin-Regensburg Cluster of Excellence CCE, Martin-Luther-Universität Halle-Wittenberg, D-06099 Halle (Saale), Germany.
[4]Center for Materials Innovation and Technology, VinUniversity, Hanoi, 100000, Vietnam.
[5]Institute of Physics, Johannes Gutenberg University Mainz, 55099, Mainz, Germany.

*Corresponding author(s). E-mail(s): kdl222@usf.edu; ethareja@usf.edu;
Contributing authors: kb3@usf.edu; gmpantano@usf.edu; tsaunder@uni-mainz.de; huong.pm@vinuni.edu.vn; phanm@usf.edu; y.mokrousov@fz-juelich.de; gayles@usf.edu;
†These authors contributed equally to this work.

S1. Spin-orbit interactions in noncoplannar calculations

In this Supplementary note, we derive the energy functions for evaluate magnetic interactions via noncollinear and noncoplanar calculations. To demonstrate those interaction, we first consider the magnetic spin configurations as follow:

$$S_i = |S| \begin{bmatrix} \cos(\phi_i)\sin\theta_i \\ \sin(\phi_i)\sin\theta_i \\ \cos\theta_i \end{bmatrix} \tag{1}$$

For noncollinear interactions, we utilize the spin spiral calculation embedded in FLEUR code [1, 2], where the azimuthal angles are descripted as the following: $\phi_i = \vec{q} \cdot \vec{R}_i + \alpha_i$ with $\vec{q}$ is the spin spiral vector, $\vec{R}_i$ is the position of the i^{th} magnetic atom and α_i is the phase-shift angle.

For noncoplanar calculations, the magnetic spin can be described in a similar approach:

$$S_i = (\sin\phi_i \cos\theta_i; \sin\phi_i \sin\theta_i; \cos\theta_i) \tag{2}$$

Yet, the change of ϕ_i and θ_i depend on the alternation of angle θ as written in the following: $\theta_i = \{\pi/2 - \theta; 0; 0\}$ and $\phi_i = \{0; \theta - \theta\}$.

Under the change of spin-orbit coupling (SOC), we consider the following magnetic interactions in the scheme of Co magnetic atoms in the Kagome net: Dzyaloshinskii-Moriya interaction (anti-exchange interaction), magnetocrystalline anisotropic energy, and spin-chiral interaction (one of the topological-chiral interactions that arise from the formation of more than two magnetic atoms [3]). To investigate the contribution of these magnetic interactions in our shandite system, we consider the following energy functional:

$$E_{SOC} = E_{SCI} + E_{MAE} + E_{DMI}$$

Firstly, we take into account the spin-chiral interaction which originate from the relativistic spin-orbit interaction coupling between magnetic spin of Co atoms) and topological orbital moment generated from the finite chirality products $\chi_{ijk} = S_i \cdot (S_j \times S_k)$ arise from the Kagome net [3]. Hence, the energy function can be written as:

$$E_{SCI} = -\sum_{i(jk)} \chi^{SO} \kappa^{TO} [\vec{S}_i (\vec{S}_j \times \vec{S}_k)](\vec{\tau}_{ijk} \cdot \vec{S}_i)$$

In addition, the direction of this magnetic interaction reply on the surface normal of the Kagome net $\tau_{ijk} \sim -const \cdot (0, 0, 1)$ which lie along the z-axis in our shandite system. Therefore, with our spin configuration as discussed in the Method section, the scalar chirality product χ_{ijk} can be descripted as follow:

$$\chi_{ijk} = \left(0, 0, \cos\left(\frac{\pi}{2} - \theta\right)\right) \cdot \left[\left(\cos\frac{\theta}{2}, \sin\frac{\theta}{2}, 0\right) \times \left(\cos\left(-\frac{\theta}{2}\right), \sin\left(-\frac{\theta}{2}\right), 0\right)\right]$$

$$= (0, 0, \sin\theta) \cdot \left(0, 0, -2\cos\frac{\theta}{2}\sin\frac{\theta}{2}\right) = -\sin^2(\theta)$$

Hence, the spin-chiral interaction can be written as follow:

$$\sum_{i(jk)} [\vec{S}_i (\vec{S}_j \times \vec{S}_k)](\vec{\tau}_{ijk} \cdot \vec{S}_i) = \left(0, 0, \cos\left(\frac{\pi}{2} - \theta\right)\right) \cdot \left(-\sin^2\theta\right) = -\sin^3\theta$$

Because surface normal of the Kagome net is pointing along the z-direction in Cartesian coordinate, the only spin that spun out-of-plane Co_1 with $\vec{S}_1 = \left(0, 0, \cos\left(\frac{\pi}{2} - \theta\right)\right)$. This lead to the energy function of spin-chiral interaction can be expressed as

$$E_{SCI} = \chi^{SO}\kappa^{TO}\sin^3\theta$$

The magneticrystalline anisotropic energy along z-direction can be written as following:

$$E_{MAE} = -K_1\left[1 - \cos^2(\theta)\right]$$

where K_1 is the dominant term in MAE as indicated in the main text. In addition, since only Co_1 has out-of-plane components $\vec{S}_1 = \left(0, 0, \cos\left(\frac{\pi}{2} - \theta\right)\right)$, we simplify the contribution of K_1 of E_{MAE} is only one-third compared to the strength of MAE indicated in the main text.

Thirdly, DM energy variation can be described as the following:

$$E_{DMI} = \sum_{ij} \vec{D}_{ij}\vec{S}_i \times \vec{S}_j$$

With the spin orientation as indicate in the Method section, we obtain the contribution of DMI along z direction as:

$$E_{DMI} = -D\sin(\theta)$$

From here, we obtain the fitting energy function for our shandite system as following:

$$E = \chi^{SO}\kappa^{TO}\sin^3\theta - K_1\sin^2\theta - D\sin\theta$$

S2. Band structures and DOS of magnetic Weyl nodes

We observe the Weyl nodes in the ferromagnetic states of Co_3Sn_2SeS compound. Up to $\phi = 72^\circ$, the magnetic Weyl nodes still remain a Type-I crossing. Until $\phi = 108^\circ$, the double-crossing feature in its electronic band structure emerged.

Under homogenous spin spiral, magnetic Weyl cones in $Co_3Sn_2Se_2$ demonstrate a similar trend compared to that in $Co_3Sn_2S_2$. Topological phase transitions occur from Type-I ($\phi = 0^\circ$) to Type-II ($\phi = 72^\circ$) and ultimately reach gapped state ($\phi = 108^\circ$).

In the case of q=[1,1,0] direction, we observe that the magnetic Weyl crossings reached gapped state in smaller angle ϕ as $\phi \geq 60^\circ$ for all shandite compounds. However, under the spin-spiral propagation q=[1,1,1], the behavior of Weyl crossing in all shandite compounds are similar to the q=[1,0,0] case as indicated in the main text.

We demonstrate the change in energy in red and blue color. Black lines indicate the energy bands without the effect of SOC. Red/blue dots indicate energy bands are shifted up/down, respectively. The size of dots display how much the energy bands changed compared to the electronic bands without SOC.

For a small angle of rotation, the energy bands describing the Weyl nodes remain unchanged. In the case of finite rotation, the bands below the Weyl nodes appear to shift downward in energy below $-0.5\ eV$ and significantly flatten, where the bands above also shift downward forming extra crossings in the region of Weyl cones. The effect of SOC perturbation does not gap the bands.

References

[1] Wimmer, E., Krakauer, H., Weinert, M. & Freeman, A. J. Full-potential self-consistent linearized-augmented-plane-wave method for calculating the electronic structure of molecules and surfaces: o_2 molecule. *Phys. Rev. B* **24**, 864–875 (1981).

[2] The FLEUR project. https://www.flapw.de/.

[3] Grytsiuk, S. *et al.* Topological–chiral magnetic interactions driven by emergent orbital magnetism. *Nature communications* **11**, 511 (2020).

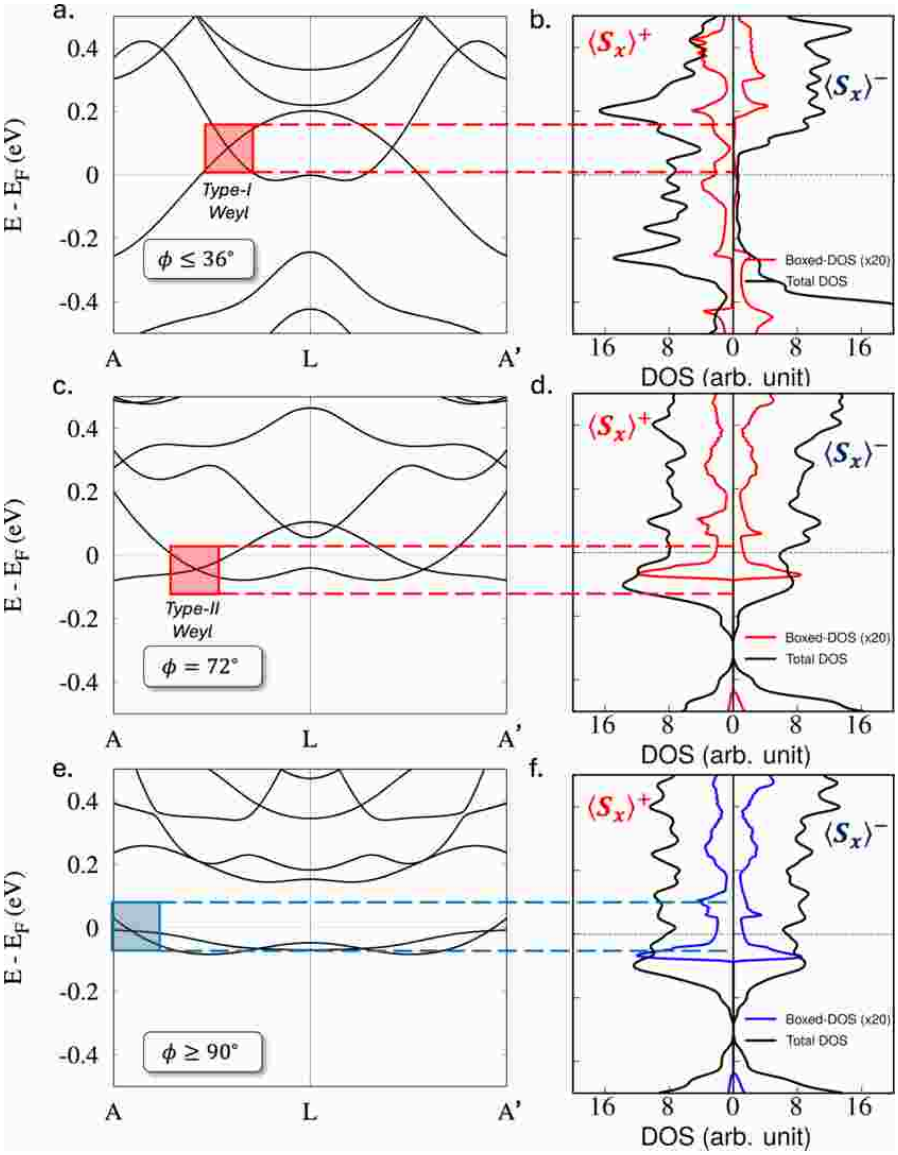

Supplementary Figure S1 Electronic band structures and density of states (DOS) of Co_3Sn_2SeS with different homogeneous spin spiral angle ϕ as indicated in previous section. Band structure and DOS are illustrated for $\phi = 0^\circ$ in (a-b), $\phi = 72^\circ$ in (c-d) and $\phi = 108^\circ$ in (e-f), respectively. The left and right panel in DOS are spin projection along the x-direction.

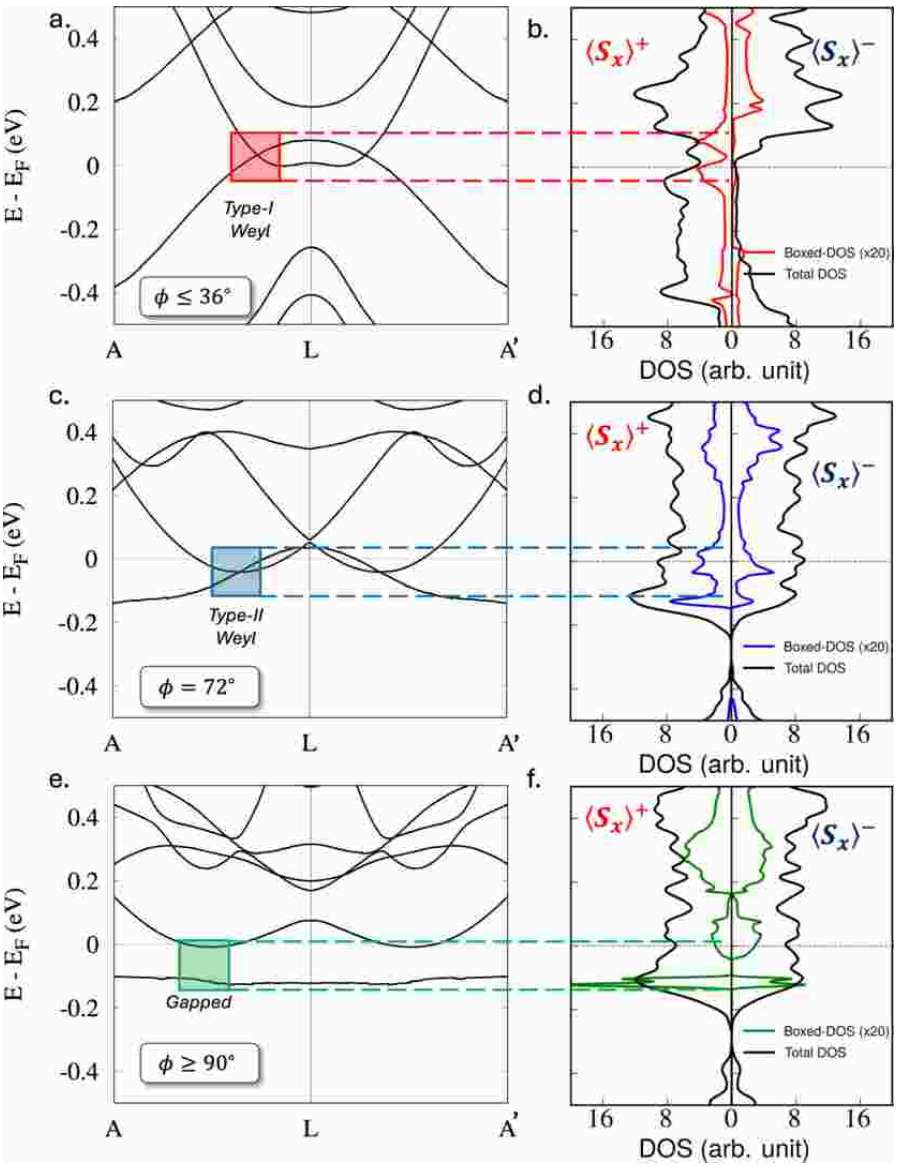

Supplementary Figure S2 Electronic band structures and density of states (DOS) of $Co_3Sn_2Se_2$ with different homogeneous spin spiral angle ϕ as indicated in previous section. Band structure and DOS are illustrated for $\phi = 0°$ in (a-b), $\phi = 72°$ in (c-d) and $\phi = 108°$ in (e-f), respectively. The left and right panel in DOS are spin projection along the x-direction.

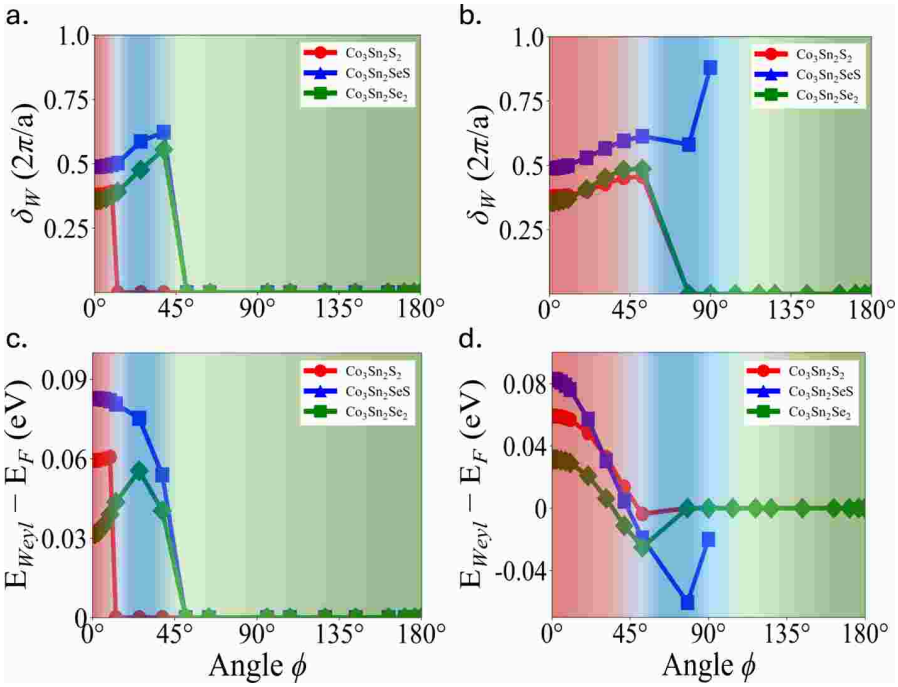

Supplementary Figure S3 Topological phase transitions of $Co_3Sn_2S_{2-x}Se_x$ are revealed, where $Co_3Sn_2S_2$, Co_3Sn_2SeS, and $Co_3Sn_2Se_2$ are in red, blue and green lines, respectively. (a,b) Distance between two Weyl crossings is plotted as a function of the spin spiral angle ϕ (along the direction q = [1, 1, 0] and q = [1, 1, 1], respectively. (c,d) Position of the Weyl pairs with respect to the Fermi energy as a function of both the mentioned directions.

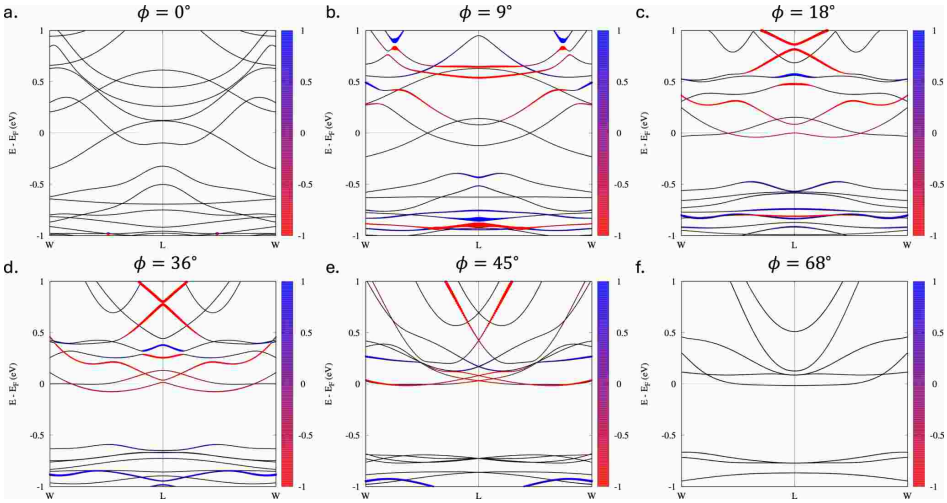

Supplementary Figure S4 Electronic band structure of Co_3Sn_2SeS under the influence of SOC. Band structure showing Weyl nodes are illustrated for (a) $\phi = 0°$, (b) $\phi = 18°$, (c) $\phi = 36°$, (d) $\phi = 72°$, (e) $\phi = 90°$ and (f) $\phi = 136°$.